Chemical Engineering Journal 140 (2008) 609–613

Chemical Engineering Journal

www.elsevier.com/locate/cej

Short communication

Effects of process variables on kinetics of methylene blue sorption onto untreated guava (*Psidium guajava*) leaf powder: Statistical analysis

V. Ponnusami*, R. Madhuram, V. Krithika, S.N. Srivastava

School of Chemical and Biotechnology, SASTRA University, Thirumalaisamudram, Thanjavur 603402, India

Received 8 August 2007; received in revised form 21 October 2007; accepted 4 November 2007

Abstract

The sorption of methylene blue onto untreated guava leaf powder has been studied. The kinetics of sorption of methylene blue is described by pseudo-second-order model. Effects of initial dye concentration, solution temperature, and adsorbent dosage have been studied. The pseudo-second-order rate constant has been correlated as a function of the system variables. Statistical tools like Student's *t*-test, *F*-test, ANOVA and lack of fit have been employed to determine the significance of each coefficient that appeared in the model. Model adequacy has been checked by residual distribution. The proposed model explains 95.1% of the total variation in the response.

Keywords: Methylene blue; Guava leaf powder; Statistical analysis; Sorption rate constant

1. Introduction

Dyes are widely used in textile, plastic, leather, and many other industries to color their end products. Considerable amount of these dye are not consumed in the process and appear in the effluent. Many of the dyes are toxic to aquatic life and even affect food chain. Therefore it becomes necessary to treat these effluents for environmental protection [1]. Some of the biological or physico-chemical treatments employed for the treatment of dye effluents include anaerobic/aerobic treatment, coagulation, flocculation, oxidation, membrane separation and sorption [2]. However, adsorption is considered to be superior to other techniques due to its low cost, simplicity of design, high decontamination efficiency and ability to treat dyes in more concentrated forms [3]. Adsorption also eliminates the need for huge sludge-handling processes [4]. Activated carbon as sorbent has been used over decades. High operating cost and problems with regeneration hamper the use of activated carbon for large-scale application [2,3]. This has lead many researchers to search for cheaper substitutes such as coal, fly ash, silica gel, wool wastes, agricultural wastes, wood wastes and many other low-cost materials [3].

Isotherm and kinetics of adsorption of several dyes on different low-cost adsorbents had been extensively studied by several researchers. In order to design appropriate sorption systems it is essential to predict the kinetics of adsorption. Most of the adsorption systems follow pseudo second order kinetics. Many researchers have shown that the second order rate constant varies with process variables like initial dye concentration (C_0), adsorbent dosage (D) and solution temperature (T). But only a few have studied the dependence of rate constant on these process variables. Ho and McKay [5,6] have expressed K_2 in terms of C_0 and D. Vadivelan and Vasanth Kumar [7] have expressed K_2 in terms of C_0. Ho et al. [8] have developed a general empirical relationship between K_2 and the process variables C_0, T, particle size and speed of agitation. The objectives of the present investigation are to establish how the process variables interacted and ultimately affected the rate constant and to develop a semi empirical correlation for the rate constant in terms of the process variables.

The adsorbate methylene blue (MB, chemical formula: $C_{16}H_{18}N_3SCl$; FW: 319.86 g mol^{-1}, λ_{max}: 662 nm, class: thiazine, C.I. classification number: 52015.) was chosen as a model dye because of its well-known adsorption characteristics. The dye is not regarded as acutely toxic, but it can have various harmful effects. Workers handling methylene blue are at risk for photoirritant contact dermatitis (PICD) [9]. High concentration of solid dye in contact with eye has been known to have caused corneal and conjunctival injury in human beings [10].

---

* Corresponding author. Tel.: +91 99947 12632; fax: +91 4362 264120.
E-mail address: vponnu@chem.sastra.edu (V. Ponnusami).

1385-8947/$ – see front matter © 2007 Elsevier B.V. All rights reserved.
doi:10.1016/j.cej.2007.11.003

Nomenclature

C_0	initial concentration of MB in the solution (mg/dm^3)
C_t	concentration of MB in the solution at time t (mg/dm^3)
D	amount of adsorbent added to the solution (g/dm^3)
K_2	second order rate constant (g mg^{-1} min^{-1})
$K_{2\text{mol}}$	second order rate constant (g mol^{-1} min^{-1})
N	dimensionless number, 1000 D/C_0
q_t	dye uptake at time t (mg/g)
t	time (min)
T	temperature (K)
X_i	process variable
X_1	ln N
X_2	reciprocal of absolute temperature (K^{-1})
x_i	dimensionless coded value for X_i
Y	response variable, $\ln K_{2\text{mol}}$

Greek symbols

β_0	global mean
β_i	linear effect
β_{ii}	quadratic effect
β_{ij}	interaction effect

Guava or *Psidium guajava* of Myrtaceae family is used as adsorbent. In our earlier report we have shown that guava leaf powder (GLP) possess excellent adsorption capacity for the removal of MB from aqueous solutions [11]. It is a tropical and semitropical plant. It is common in backyards and waste places. The raw leaves contain fixed oil 6%, and volatile oil 0.365%, resin 3.15%, tannin 8.5%, and a number of other fixed substances. Its seeds and leaves possess medicinal value and are traditionally used to treat a number of human ailments [12].

The factorial experimental design involves changing all variables (factors) from one experiment to the next. It determines which factors have important effects on the dependent variable (response) as well as interactions between the factors. Either a linear or a quadratic regression model is used to explain the behavior of the system under study. The significance of each coefficient in the model is determined by Student *t*-test and *p*-values. The variability in dependent variables is explained by the multiple regression coefficient of determination, R^2. Adequacy of the model is tested by analysis of variance (ANOVA) and lack of fit [13–15].

2. Experimental

2.1. Materials

Mature guava leaves were washed thoroughly with distilled water to remove dust and other impurities and dried at 343 K in hot air oven overnight. Dried leaves were then ground, screened to desired size, washed and dried again. Dried GLP was stored in plastic containers for further use. BSS#—100+150 size particles were used in the present study. The Laboratory grade MB dye was obtained from Himedia India Limited, and used without further purification. A stock solution was prepared by dissolving required amount of dye in double distilled water which was later diluted to required concentrations. All the solutions were prepared in double distilled water. Solution pH was not adjusted as natural pH was favorable for the chosen system [11]. Concentrations of the dye solutions were determined by measuring the absorbance of the solution at the characteristic wavelength ($\lambda_{\max} = 662$ nm) of MB using a double beam UV–vis. spectrophotometer (Systronics 2201). Samples were diluted if the absorbance exceeds 0.8. Final concentration was then determined from the calibration curve.

Dye uptake was calculated using the following formula

$$q_t = \frac{(C_0 - C_t)}{D} X100 \tag{1}$$

2.2. Kinetics

Required amount of guava leaf powder was added to 100 ml dye solution of required concentration taken in 250 ml conical flask. Flasks were then kept in an incubated shaker and agitated at 200 rpm. Samples taken at regular time intervals were filtered and concentration of dye in the filtrates were determined using UV–vis. spectrophotometer.

The kinetic rate data were analyzed using Ho's second order expression [4,5,16]

$$\frac{t}{q_t} = \frac{1}{K_2 q_e^2} + \frac{t}{q_e} \tag{2}$$

Plot of t/q_t vs. t is straight line. From the slope and intercept of the plot rate constant and maximum dye uptake can be determined. Batch experiments were conducted by varying concentration (100, 200 and 300 mg/dm^3), dosage (1, 2 and 3 g/dm^3) and temperature (293, 308 and 323 K) one at a time. Thus a total of 27 experiments were conducted. The rate constant for each run was determined using Ho's second order rate expression (Eq. (2)).

3. Results and discussion

Experimental results are given in Table 1. Results were analyzed using Minitab 14. For the analysis of data, dimensionless number N was defined as D/C_0 and $\ln N$ was used as a factor (X_1) in the model. In analogous with Arhenius theory reciprocal of the temperature was used as another factor (X_2) in the model. Also, for statistical calculations, the variables X_i were coded as x_i according to the following relationship.

$$x_i = \frac{(X_i - X_0)}{\Delta X} \tag{3}$$

Codified mathematical model employed for the custom design was

$$Y = \beta_0 + \sum \beta_i x_i + \sum \beta_{ii} x_i^2 + \sum \beta_{ij} x_i x_j \tag{4}$$

Table 1
Experimental data

Sl. no.	ln(N)	$1/T$ (K^{-1})	ln $K_{2\text{mol}}$
1	3.4012	0.003096	9.524
2	3.4012	0.003247	8.432
3	3.4012	0.003413	7.960
4	2.7081	0.003096	7.164
5	2.7081	0.003247	7.236
6	2.7081	0.003413	6.068
7	2.3026	0.003096	5.658
8	2.3026	0.003247	7.011
9	2.3026	0.003413	4.960
10	2.9957	0.003096	6.947
11	2.9957	0.003247	7.508
12	2.9957	0.003413	6.662
13	2.3026	0.003096	5.616
14	2.3026	0.003247	6.250
15	2.3026	0.003413	5.328
16	1.8971	0.003096	4.330
17	1.8971	0.003247	5.065
18	1.8971	0.003413	4.646
19	2.3026	0.003096	5.149
20	2.3026	0.003247	5.248
21	2.3026	0.003413	5.073
22	1.6094	0.003096	4.096
23	1.6094	0.003247	4.852
24	1.6094	0.003413	4.462
25	1.2040	0.003096	3.928
26	1.2040	0.003247	4.358
27	1.2040	0.003413	5.130

The main effects of the factors were first determined. The effect of a factor is defined as the change in response produced by a change in the level of the factor. The regression coefficient, the associated standard errors and effects are shown in Table 2. Substituting the regression coefficients in Eq. (4) and rearranging, we get:

$$K_{2\text{mol}} = 362.6362N^{a_1}\ \exp(-a_2) \tag{5}$$

where $a_1 = 2.134 + 0.9382x_1 - 0.6018x_2$ and $a_2 = 0.1179x_2 + 0.5076x_2^2$

The results fit the data well. Model explains 92.5% of the total variation in the response ($R^2 = 92.5\%$). Statistical significance of the each coefficient in the model was determined by the Student's *t*-test and *p*-values. Table 3 show the sum of squares used to estimate the factors' effect and the *F*-ratios. *F*-ratios are defined as the ratio of the respective mean-square-effect and the mean-square-error. The small value of p (less than 0.05) indicated the significance of the model terms. The non-significant value of lack of fit ($p = 0.871$) indicated that the quadratic model was valid for the present study.

Table 2
Estimated regression coefficients for ln $K_{2\text{mol}}$

Term	Coefficient	S.E. coefficient	T	p
Constant	5.8934	0.1648	35.765	0.000
$1/T$	−0.1179	0.1033	−1.142	0.266
ln(N)	2.1340	0.1445	14.773	0.000
$1/T \times 1/T$	−0.5076	0.1794	−2.830	0.010
ln(N) × ln(N)	0.9382	0.2212	4.241	0.000
$1/T \times$ ln(N)	−0.6018	0.1768	−3.404	0.003

S = 0.4382; $R^2 = 92.5\%$; R^2(adj.) = 90.7%.

Table 3
Analysis of variance for ln $K_{2\text{mol}}$

Source	d.f.	Seq. SS	Adj. SS	Adj. MS	F	p
Regression	5	49.808	49.808	9.9617	51.88	0.000
Linear	2	42.592	42.155	21.0774	109.77	0.000
Square	2	4.991	4.991	2.4956	13.00	0.000
Interaction	1	2.225	2.225	2.2247	11.59	0.003
Residual error	21	4.032	4.032	0.1920		
Lack-of-fit	15	2.238	2.238	0.1492	0.50	0.871
Pure error	6	1.794	1.794	0.2991		
Total	26	53.841				

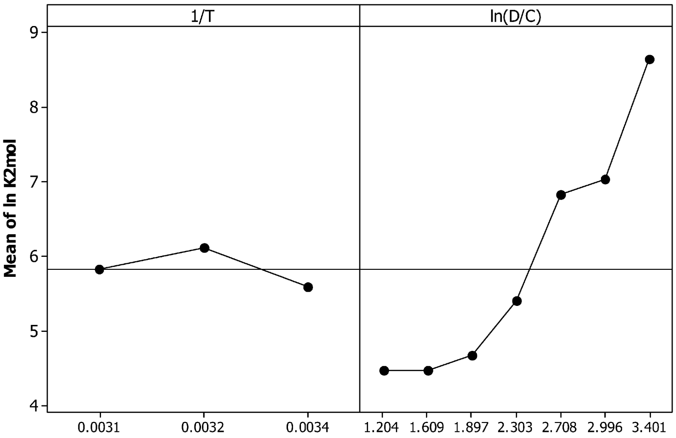

Fig. 1. Main effects plot for ln $K_{2\text{mol}}$.

Main effect plot is shown in Fig. 1. The curves in the figure indicate that both N and $1/T$ have quadratic effect on the rate constant. Corresponding *p*-values of the quadratic terms in the ANOVA table (Table 3) are less than 0.05. This confirms the fact that the variables N and $1/T$ have quadratic effect on the response variable.

We should also examine the residual distribution to check the adequacy of the model. Residuals are the difference between the predicted and experimental values [13]. The normal probability plot of residual values can be used to identify possible outliers. The plot is shown in Fig. 2. Run number 8 (corresponding to $T = 293$ K, $C_0 = 200$ mg/dm^3 and $D = 3$ g/dm^3) was found to be

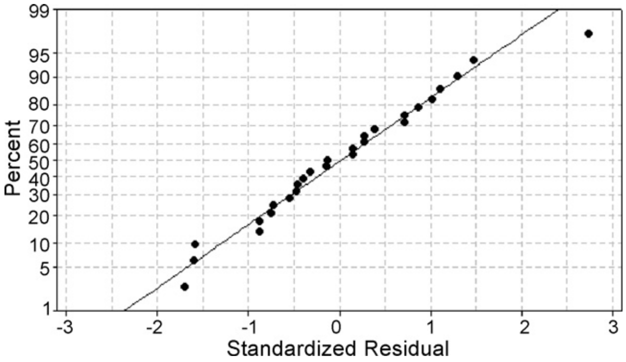

Fig. 2. Normal probability plot of residual values for ln $K_{2\text{mol}}$.

Table 4
Estimated regression coefficients for $\ln K_{2\text{mol}}$ (without outlier)

Term	Coefficient	S.E. coefficient	T	p
Constant	5.7107	0.14599	39.118	0.000
$1/T$	−0.1179	0.08483	−1.390	0.180
$\ln(N)$	2.1340	0.11864	17.987	0.000
$1/T \times 1/T$	−0.3633	0.15355	−2.366	0.028
$\ln(N) \times \ln(\mathrm{N})$	1.0508	0.18480	5.686	0.000
$1/T \times \ln(N)$	−0.6018	0.14522	−4.144	0.001

$S = 0.3599$; $R^2 = 95.1\%$; $R^2(\text{adj.}) = 93.8\%$.

the possible outlier. After elimination of the outlier main effects and interactions were recalculated and the results are shown in Table 4. R^2 was 95.1% for regression model without outlier. That is the model explains 95.1% of the total variation in the response leaving only 4.9% to the residuals. This confirms that the data point was a real outlier. Substituting the regression coefficients in Eq. (4) and rearranging, we get

$$K_{2\text{mol}} = 302.0825 N^{a_1} \exp(-a_2) \qquad (6)$$

where $a_1 = 2.134 + 1.0508x_1 - 0.6018x_2$ and $a_2 = 0.1179x_2 + 0.3633x_2^2$

Thus, $K_{2\text{mol}}$ can be predicted for any set of process system variables. From the results it is evident that the interaction between $\ln N$ and $1/T$, second order main effect of $\ln N$ and second order main effect of $1/T$ were all found to be statistically significant. In conventional experimental analysis these significant interaction and quadratic effects would have been lost [14]. The model also makes it possible to predict the response surface. The response surface and contour plot are shown in Figs. 3 and 4. Curved surfaces in the contour and surface plots confirm the interaction between $\ln N$ and $1/T$.

As mentioned earlier many researchers have reported that K_2 value varies with initial dye concentration, adsorbent dosage and temperature. Though it was not possible to compare the present results directly with the previous reports the general trends could be compared. From Fig. 1 it can be seen that value of $\ln K_{2\text{mol}}$ increased with increase in $\ln N$. That is $\ln K_{2\text{mol}}$ value increase with increase in D and decrease with increase in C_0. Also, it can be seen that the value of $\ln K_{2\text{mol}}$ first increases and then drops with increase in temperature.

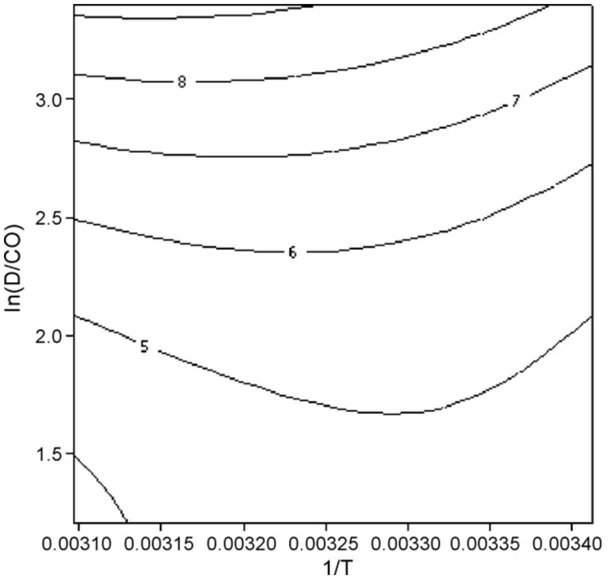

Fig. 3. Contour plot of $\ln K_{2\text{mol}}$ vs. $\ln N$ and $1/T$.

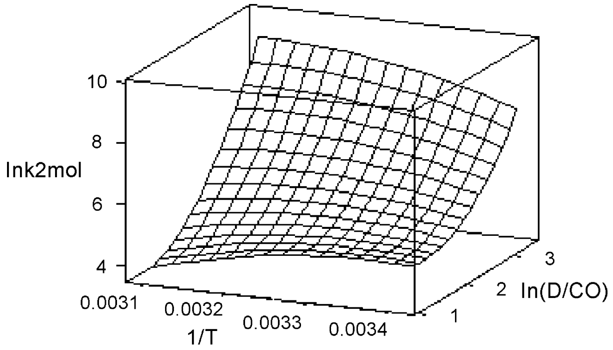

Fig. 4. Response surface plot of $\ln K_{2\text{mol}}$ vs. $\ln N$ and $1/T$.

Mane et al. [17], Yeddou and Bensmali [18], Suteu and Bilba [19], Jumasiah et al. [20], Ho et al. [8], had reported that K_2 decreased with increase in initial dye concentration. Eren and Nuran Acar [21] studied adsorption of Reactive Black 5 (RB5) onto powdered activated carbon (PAC) and fly ash. K_2 value for Fly ash–RB5 system initially increased and then decreased with increase in dye concentration. But, for PAC–RB5 system K_2 decreased with increase in dye concentration. Present findings are in good agreement with these observations.

Janos et al. [22], Yeddou and Bensmali [18] had shown similar positive trends of K_2 with adsorbent dosage. These reports also support the findings of the present study.

Bulut and Aydin [3] had reported that K_2 increased with increase in temperature. Yeddou and Bensmali [18] had reported that K_2 decreased with increase in temperature. Ho et al. [8] studied the sorption of lead ions onto tree fern and reported that K_2 value increased initial concentration of the solution.

4. Conclusion

A generalized correlation for second order rate constant in terms adsorbent dosage, initial dye concentration and temperature has been proposed. The proposed model explains 95.1% of total variation in the rate constant. The model can be used to predict the rate constant. Predicted rate constant can be used to predict the sorption kinetics of MB onto GLP and to design suitable adsorption systems.

References

[1] T.G. Chuah, A. Jumasiah, I. Azni, S. Katayon, S.Y. Thomas Choong, Rice husk as a potentially low-cost biosorbent for heavy metal and dye removal: an overview, Desalination 175 (2005) 305–316.

[2] R. Gong, Y. Jin, J. Chen, Y. Hu, J. Sun, Removal of basic dyes from aqueous solution by sorption on phosphoric acid modified rice straw, Dyes Pigments 73 (2007) 332–337.

[3] Y. Bulut, H. Aydin, A kinetics and thermodynamics study of methylene blue adsorption on wheat shells, Desalination 194 (2006) 259–267.

[4] Y.S. Ho, G. McKay, Pseudo-second order model for sorption processes, Proc. Biochem. 34 (1999) 451–465.

[5] Y.S. Ho, G. Mckay, The kinetics of sorption of divalent metal ions onto sphagnum moss peat, Water Res. 34 (2000) 735–742.

[6] Y.S. Ho, G. McKay, A kinetic study of dye sorption by biosorbent waste product pith, Resour. Conserv. Recy. 25 (1999) 171–193.

[7] V. Vadivelan, K. Vasanth Kumar, Equilibrium, kinetics, mechanism, and process design for the sorption of methylene blue onto rice husk, J. Colloid Interface Sci. 286 (2005) 90–100.

[8] Y.S. Ho, J.C.Y. Ng, G. McKay, Removal of lead(II) from effluents by sorption on peat using second-order kinetics, Sep. Sci. Technol. 36 (2001) 241–261.

[9] http://hazmap.nlm.nih.gov/cgi-bin/hazmap_generic?tbl=TblAgents&id=1026, Specialized Information Services, U.S. National Library of 623 Medicine, 20-June-2007.

[10] http://toxnet.nlm.nih.gov/cgi-bin/sis/search/r?dbs+hsdb:@term+@rn+61-73-4, Hazardous Substances Data Bank (HSDB), U.S. National Library of Medicine (NIM), 20-06-2007.

[11] V. Ponnusami, S. Vikram, S.N. Srivastava, Guava (*Psidium guajava*) leaf powder: novel adsorbent for removal of methylene blue from aqueous solutions, J. Hazard. Mater. 152 (2008) 276–286.

[12] C. Anthony, A review of Guava (*Psidium guajava*), Personal Care Mag. 6 (2005) 33–39.

[13] Enid R. Carmona Margarita, Pereira da Silva Mônica Antunes, Selma G. Ferreira Leite, Biosorption of chromium using factorial experimental design, Proc. Biochem. 40 (2005) 779–788.

[14] V. Ponnusami, V. Krithika, R. Madhuram, S.N. Srivastava, Biosorption of reactive dye using acid-treated rice husk: factorial design analysis, J. Hazard. Mater. 142 (2007) 397–403.

[15] J. Devore, N. Farnum, Applied Statistics for Engineers and Scientist, Duxbury press, Pacific Grove, CA, USA, 1999.

[16] Y.S. Ho, G. McKay, Sorption of dye from aqueous solution by peat, Chem. Eng. J. 70 (1998) 115–124.

[17] V.S. Mane, I.D. Mall, V.C. Srivastava, Use of bagasse fly ash as an adsorbent for the removal of brilliant green dye from aqueous solution, Dyes Pigments 73 (2007) 269–278.

[18] N. Yeddou, A. Bensmaili, Kinetic models for the sorption of the dye from aqueous solution by clay–wood sawdust mixture, Desalination 185 (2005) 499–508.

[19] D. Suteu, D. Bilba, Equilibrium and kinetic study of Reactive Brilliant Red HE-3B adsorption by activated charcoal, Acta. Chim. Slov. 52 (2005) 73–79.

[20] A. Jumasiah, T.G. Chuah, J. Gimbon, T.S.Y. Choong, I. Azni, Adsorption of basic dye onto palm kernel shell activated carbon: sorption equilibrium and kinetics studies, Desalination 186 (2005) 57–64.

[21] Z. Eren, F. Nuran Acar, Adsorption of Reactive Black 5 from an aqueous solution: equilibrium and kinetic studies, Desalination 194 (2006) 1–10.

[22] P. Janoš, P. Michálek, L. Turek, Sorption of ionic dyes onto untreated low-rank coal—oxihumolite: A kinetic study, Dyes Pigments 74 (2007) 363–370.